Gut cannabinoid receptor 1 regulates alcohol binge-induced intestinal permeability

Luca Maccioni ![ORCID] ,[1,2] Szabolcs Dvorácskó ![ORCID] ,[2,3,4,5] Grzegorz Godlewski ![ORCID] ,[2] Resat Cinar ![ORCID] ,[3] Malliga R Iyer ![ORCID] ,[4] Bin Gao ![ORCID] ,[1] George Kunos ![ORCID] [2]

ABSTRACT

Background Endocannabinoids acting via cannabinoid receptor 1 (CB1R) can elicit increased intestinal permeability (a condition also called 'leaky gut'). Alcohol binge can adversely affect digestive functions, including intestinal permeability; however, the underlying mechanisms remain incompletely understood. The current study aimed at examining whether CB1R is involved in alcohol binge-induced intestinal permeability.
Methods We developed intestinal epithelial-specific CB1R knockout (CB1$^{IEC-/-}$) mice and evaluated the *in vivo* contribution of gut CB1R in alcohol binge-induced intestinal permeability.
Results Alcohol binge increased anandamide levels in the proximal small intestine in association with increased intestinal permeability. Radioligand binding and functional assays confirmed that the genetic deletion of intestinal epithelial CB1R did not alter the density or functionality of CB1R in the brain. Additionally, a peripheral CB1R antagonist, (*S*)-MRI-1891 (INV-202/monlunabant), exhibited comparable binding affinity to CB1R in brain homogenates. An acute oral administration of (*S*)-MRI-1891 (3 mg/kg) reduced alcohol binge-induced intestinal permeability in littermate control CB1$^{f/f}$ (CB1 floxed/floxed) mice but had no effect in CB1$^{IEC-/-}$ mice, underscoring the role of intestinal CB1R in this phenomenon. Mechanistically, we found that alcohol activated intestinal epithelial CB1R-ERK1/2 pathway with subsequent downregulation of tight junction proteins and reduction in villi length. In addition, targeting intestinal CB1R and downstream ERK1/2 was able to reverse this process, with subsequent upregulation of tight junction proteins and increased villi length, thus improving gut barrier function. Despite the effects on intestinal permeability, deletion of intestinal CB1R did not significantly affect metabolic parameters and liver disease.
Conclusion Our findings suggest that alcohol promotes leaky gut via the activation of gut epithelial CB1R and demonstrate that inhibition of CB1R with peripheral-restricted selective CB1R antagonists can prevent alcohol binge-induced intestinal permeability.

WHAT IS ALREADY KNOWN ON THIS TOPIC

⇒ Alcohol binge can increase intestinal permeability.
⇒ Activation of the gut cannabinoid receptor 1 (CB1R) inhibits intestinal motility and secretions; however, its role in alcohol binge-induced intestinal permeability has not been explored.

WHAT THIS STUDY ADDS

⇒ Alcohol binge increases endocannabinoids levels in the proximal small intestine and activates epithelial CB1R.
⇒ Activation of CB1R-ERK1/2 pathway links alcohol binge with tight junction disruption and changes in villus differentiation.
⇒ Genetic or pharmacological inhibition of intestinal epithelial CB1R restores alcohol binge-induced intestinal permeability.

HOW THIS STUDY MIGHT AFFECT RESEARCH, PRACTICE OR POLICY

⇒ Peripheral CB1R antagonism may be considered a novel therapeutic modality for treating alcohol-associated leaky gut and its pathological consequences.

INTRODUCTION

Alcohol is a leading cause of death, with more than three million deaths per year linked to alcohol misuse.[1] Heavy alcohol consumption can promote a plethora of diseases, including digestive diseases. According to a recent report of the World Health Organization, digestive diseases caused by the alcohol-related disorders have high rate of mortality.[1] Despite alcohol-associated gastrointestinal diseases (AGD) representing a major public health issue worldwide, there are no Food and Drug Administration-approved drugs for their treatment and their pathophysiology is not completely understood.

The risk of development of AGD is associated with the quantity of alcohol consumed and with the pattern of drinking.[2] Binge drinking is defined as a pattern of drinking that results in blood alcohol concentration of 0.08 g/dL or more, which means five or more drinks for men and four or more drinks for women within 2 hours, or approximately 0.8–1.0 g/kg in a 70 kg subject.[3] Binge drinking is a principal risk factor for the development of AGD,

such as alcohol-associated bowel disease (ABD).[4] Factors that contribute to ABD pathogenesis include increased intestinal permeability (a process also known as 'leaky gut'),[5] changes in the gut microbiome[6] and dysfunctions of the intestinal immune system.[7]

The endocannabinoid system is known to modulate intestinal functions.[8 9] Activation of the endocannabinoids receptors in the intestine inhibits intestinal motility,[10] modulates gut immunity,[11] affects food intake[12] and regulates intestinal permeability.[13] Interestingly, a recent study has shown that cannabinoid receptor 1 (CB1R) regulates obesity-related intestinal permeability in mice.[14] Another study suggests that inhibition of CB1R can reduce alcohol-induced translocation of lipopolysaccharide (LPS).[15] However, the mechanistic involvement of gut CB1R in alcohol-induced intestinal permeability has not been investigated.

Here we provide *in vivo* evidence of the role of intestinal epithelial CB1R in alcohol-induced intestinal permeability. Genetic deletion or pharmacological inhibition of intestinal CB1R reduced alcohol binge-induced intestinal permeability via a CB1R-ERK1/2 pathway. Our results shed light on the role of gut epithelial CB1R in alcohol-induced leaky gut and suggest that peripheral-restricted CB1R antagonists may be used for the treatment of alcohol binge-related intestinal permeability and its pathological consequences.

MATERIALS AND METHODS

Mice

Mice were housed in polycarbonate cages (four or fewer mice per cage) and maintained in a temperature-controlled and light-controlled facility (12:12 light–dark cycle) under standard food and water ad libitum. C57BL/6J (JAX:000664) and VillinCre (JAX:004586) mice were purchased from The Jackson Laboratory. CB1 floxed/floxed (CB1$^{f/f}$) mice were originally obtained from Dr Josephine M Egan (National Institute on Aging, National Institutes of Health).[16] C57BL/6J mice were used for measurements of intestinal endocannabinoids. VillinCre mice were crossed with CB1$^{f/f}$ via several steps to generate intestinal epithelium-specific (CB1$^{IEC-/-}$) deletion of CB1R and littermate control mice: VillinCre negative-CB1$^{f/f}$ (referred to as CB1$^{f/f}$ in the manuscript). We followed the ARRIVE (Animal Research: Reporting of *In Vivo* Experiments) guidelines for reporting preclinical animal studies.

Endocannabinoids extraction and measurement

Endocannabinoids were extracted and quantified by liquid chromatography-tandem mass spectrometry (LC-MS/MS) as previously described.[17] Briefly, intestinal tissues were collected as follows: duodenum around 1 cm after the pylorus, jejunum around 3 cm after the ligament of Treitz, terminal ileum 1 cm near the entry into the caecum and colon as the mid-distal part of the colon. Intestinal tissues were homogenised in 0.5 mL of ice-cold methanol/Tris buffer (50 mM, pH 8.0), 1:1, containing 7 ng of [^{2}H$_4$]-arachidonoyl ethanolamide and [^{2}H$_5$]-2-arachidonoylglycerol as internal standards. Homogenates were extracted three times with CHCl3:methanol (2:1, vol/vol), dried under nitrogen and reconstituted with methanol after precipitating proteins with ice-cold acetone. LC-MS/MS was performed on an Agilent 6470 triple quadrupole mass spectrometer (Agilent Technologies) coupled to an Agilent 1200 LC system. Levels of endocannabinoids in the samples were measured against standard curves using MassHunter Workstation LC/QQQ Acquisition and MassHunter Workstation Quantitative Analysis software (Agilent Technologies). Values are expressed as pmol or nmol/g wet tissue.

Preparation of brain membrane homogenates

Preparation of CB1$^{f/f}$ and CB1$^{IEC-/-}$ mouse brain tissue membrane homogenates was performed as previously described.[18 19] Briefly, crude membrane fractions were prepared from the brain without the cerebellum. CB1$^{f/f}$ and CB1$^{IEC-/-}$ mouse brains were quickly removed from the euthanised mice and placed directly into ice-cold 50 mM Tris-HCl buffer (pH 7.4). The collected tissue was then homogenised in 30 volumes of ice-cold buffer using a Braun Teflon glass homogeniser at the highest revolutions per minute (rpm). The homogenate was centrifuged at 48 000× *g* for 20 min at 4°C and the resulting pellet was suspended in the same volume of a cold buffer and homogenised. Centrifugation was then repeated. The final pellets were resuspended in five volumes of 50 mM Tris-HCl (pH 7.4) and stored at −80°C. Prior to the experiment, aliquots were thawed, homogenised with a Dounce homogeniser and the protein concentration determined by the Pierce BCA Protein Assay Kit (ThermoFisher). Samples were then diluted to obtain the appropriate amount for the assay.

Radioligand saturation binding assay

Saturation binding experiments were carried out at 30°C for 60 min in a 50 mM Tris-HCl (1 mM EDTA, 3 mM MgCl$_2$, 1 mg/mL bovine serum albumin (BSA)) binding buffer (pH 7.4) in silanised glass tubes in a total assay volume of 1 mL. The experiments were performed by measuring the specific binding of [^{3}H]-CP55.940 (0.10–11.9 nM) to 0.5 mg/mL brain membrane homogenates from CB1$^{f/f}$ and CB1$^{IEC-/-}$ mice to determine the equilibrium dissociation constant (K$_d$) and the maximal number of binding sites (B$_{max}$). The specific binding was measured in the presence of 10 µM CP55,940.

Radioligand competition binding assay

Binding experiments were performed at 30°C for 60 min in a 50 mM Tris-HCl (1 mM EDTA, 3 mM MgCl$_2$, 1 mg/mL BSA) binding buffer (pH 7.4) in silanised glass tubes in a total assay volume of 1 mL that contained 0.5 mg/mL of membrane protein. Competition binding experiments were carried out by incubating cell membranes with 0.5 nM of [^{3}H]-CP55.940 (K$_d$: 1.68 nM of CB1$^{f/f}$ and

1.7 nM of CB1$^{IEC-/-}$ mice) in the presence of increasing concentrations (10^{-12}–10^{-6} M) of unlabelled ligands. Non-specific binding was determined in the presence of 10 µM of CP55.940. The incubation was terminated by diluting the samples with an ice-cold wash buffer (50 mM Tris-HCl, pH 7.4, 1 mg/mL BSA), followed by repeated washing and rapid filtration through Whatman GF/B glass fibre filters (Whatman, Maidstone, England). Filtration was performed with a 24-well Brandel Cell Harvester (Gaithersburg, Maryland, USA). Filters were air-dried and immersed into Ultima Gold MV scintillation cocktail, and then radioactivity was measured with a Tri-Carb liquid scintillation analyser (Packard, PerkinElmer, Waltham, Massachusetts, USA).

Ligand-stimulated [^{35}S]-GTPγS binding assay

The inhibitory potencies of the antagonists in G protein signalling were measured as described previously.[19] Briefly, the inhibitory potency of the antagonist was measured by their ability to concentration-dependently inhibit the stimulation of [^{35}S]-GTPγS binding by 300 nM CP-55,940 (Sigma-Aldrich), which generated CB1R-mediated increase in [^{35}S]-GTPγS binding at ~EC80 level. CB1$^{f/f}$ and CB1$^{IEC-/-}$ mouse brain homogenate (30 µg) was incubated with 0.05 nM [^{35}S]-GTPγS (Revvity) and the indicated concentrations of ligands in TEM buffer (50 mM Tris-HCl, 0.2 mM ethylene glycerol tetraacetic acid (EGTA) and 9 mM MgCl2, pH 7.4) containing 100 µM Guanosine 5' triphosphate (GDP), 150 mM NaCl and 0.1% (w/v) bovine serum albumin in a total volume of 1 mL for 60 min at 30°C. Non-specific binding was determined in the presence of 10 µM GTPγS, and at baseline it represented <10% of total binding. Agonist-stimulated [^{35}S]-GTPγS binding was expressed as the per cent of increase over baseline. Bound and free [^{35}S]-GTPγS levels were separated by vacuum filtration through Whatman GF/B filters using a Brandel M24 Cell Harvester (Gaithersburg, Maryland). Filters were washed with ice-cold buffer, and radioactivity was detected by scintillation spectrometry (LS6500; Beckman Coulter). Dose–response curves were generated in the presence of increasing concentrations of antagonists. Concentration–response relationships were analysed by fitting the data into the three-parameter model 'log(agonist) vs response' in GraphPad Prism.

Measurement of intestinal permeability *in vivo*

Intestinal permeability was assessed as previously described.[20] Briefly, fluorescein isothiocyanate (FITC)-dextran 4 kDa (Sigma) at a dose of 600 mg/kg was given by gavage to all the mice 4 hours before sacrifice and 1 hour before the alcohol binge. FITC-dextran measurements were performed in plasma by fluorometry. The plasma concentration of the FITC-dextran was determined using a fluorimeter with an excitation wavelength of 490 nm and an emission wavelength of 530 nm. Serially diluted FITC-dextran was used to establish a standard curve, and the plasma FITC-dextran concentrations were then calculated.

Pharmacological treatment

The peripheral-restricted selective CB1R receptor antagonist (*S*)-MRI-1891 was synthesised as previously described.[21] The drug was delivered by oral gavage at the maximally effective dose of 3 mg/kg at 1.5 hours before the alcohol binge. According to our previous publication,[21] *in vivo* upper gastrointestinal motility efficacy assay, the (*S*)-MRI-1891 compound demonstrated a dose-dependent effect (0.3, 1 and 3 mg/kg), with the 3 mg/kg dose maximally antagonising CB1R agonist-induced inhibition of upper gastrointestinal motility. Furthermore, (*S*)-MRI-1891 at a 3 mg/kg dose increased upper gastrointestinal motility in the absence of a CB1R agonist, further confirming its *in vivo* CB1R inverse agonist activity. Importantly, (*S*)-MRI-1891 did not induce anxiogenic behaviour at 3 mg/kg or even at a high dose of 30 mg/kg during chronic treatment, in contrast to the brain-penetrant CB1R antagonist rimonabant, which induced significant anxiety at a dose of 3 mg/kg.[21] The mitogen activated protein kinase kinase 1/2 (MEK1/2) inhibitor U0126 (20 mg/kg; MedChemExpress) was delivered intraperitoneally 1.5 hours before the alcohol binge. Mice were sacrificed 3 hours later after the binge, and intestinal permeability *in vivo* as well as intestinal tissues were collected for further analysis.

Indirect measurement of metabolic parameters

Indirect metabolic rate measurements were conducted on an Oxymax Metabolic Cage System (Columbus Instruments) as previously described.[22] The Oxymax System is a non-invasive set-up that directly measures respiratory exchange ratio (O_2 and CO_2), as well as mouse physical activity measured by infrared beams and detectors. Total energy expenditure (TEE) was calculated as volume of oxygen consumption $(VO)_2 \times (3.815 + 1.232 \times RQ)$, where RQ is the respiratory quotient (the ratio of volume of carbon dioxide $(VCO)_2$ to VO_2). Net oxidation rates of fat and carbohydrates were calculated as previously described[23]: fat oxidation $= 1.69 \times (VO_2 - VCO_2)$; carbohydrate oxidation $= 4.57 \times VCO_2 - 3.23 \times VO_2$. Values were normalised with respect to the body weight and adjusted to an effective metabolic body size (0.75 kg).

Statistical analysis

Data were analysed using GraphPad Prism V.9 (GraphPad Software) and presented as mean±SEM unless otherwise indicated. Normality was evaluated using Kolmogorov-Smirnov, followed by t-test or Wilcoxon test as appropriate. Data from multiple groups were analysed with one-way analysis of variance, followed by Tukey's post-hoc test. A p value <0.05 was considered statistically significant.

All other materials and methods are listed in online supplemental material.

RESULTS

Measurement of gut endocannabinoids

The intestine fulfils several functions according to the site of intestinal tract.[24] We first evaluated endocannabinoids levels at different sites of the intestinal tract by LC-MS/MS (figure 1A). Our results showed very high levels of the endocannabinoid anandamide (AEA) in the duodenum of C57BL/6 mice compared with those in other parts of the small intestines. Moreover, very high levels of 2-arachidonoylglycerol (2-AG) were found in the proximal small intestine (duodenum and jejunum) (figure 1B).

Generation of intestinal-specific CB1R knockout mice

To study the functional role of intestinal endocannabinoids and their CB1R, we generated CB1$^{IEC-/-}$ knockout mice by crossing CB1$^{f/f}$ mice with VillinCre mice via several steps (figure 1C). We next aimed at validating our genetic strategy by quantitative PCR (qPCR) and pharmacologically characterising CB1R in the brain where it is expressed at very high levels. We first used qPCR quantification of *Cnr1*, the gene encoding CB1R, in isolated intestinal epithelial cells and in whole duodenal extracts and confirmed knockout of CB1R in epithelial cells and reduced duodenal CB1R expression (around 50%) in CB1$^{IEC-/-}$ mice compared with CB1$^{f/f}$ mice (figure 1D). We next pharmacologically validated our genetic strategy. The maximum binding capacity (receptor density, B$_{max}$) of the specific CB1/CB2R radioligand [^{3}H]-CP55,940 and the binding affinity (K$_i$) of (S)-MRI-1891 were determined using saturation and competitive binding assays on brain membrane homogenates from CB1$^{f/f}$ and CB1$^{IEC-/-}$ mice. In saturation binding experiments, the specific binding of [^{3}H]-CP55,940 was found to be saturable and exhibited high affinity in the nanomolar range across brain tissue homogenates (figure 1E). In radioligand competition binding assays, a selective peripheral CB1R antagonist, (S)-MRI-1891, effectively displaces the radioligand [^{3}H]-CP55,940 from the binding site, demonstrating high binding affinity in the nanomolar range on CB1$^{f/f}$ and CB1$^{IEC-/-}$ mice membrane homogenates. These findings are consistent with previously reported binding affinity results for (S)-MRI-1891.[21] No differences were observed in the inhibitory constant (K$_i$) values of (S)-MRI-1891 between CB1$^{f/f}$ and CB1$^{IEC-/-}$ mouse intestinal membrane homogenates (figure 1F). CB1R-mediated G protein activity was assessed using [^{35}S]-GTPγS binding assays to evaluate the functional antagonism of (S)-MRI-1891 on membrane homogenates from CB1$^{f/f}$ and CB1$^{IEC-/-}$ mice. On both membranes, the inhibitory potency of (S)-MRI-1891 was very similar in the presence of 300 nM of the CB1R agonist CP55,940 (figure 1G). These data support the fact that our genetic strategy did not affect central CB1R functionality, while reducing gene expression of intestinal CB1R in CB1$^{IEC-/-}$ mice by knocking it out only in epithelial cells.

Genetic deletion of intestinal CB1R ameliorates alcohol-induced and HFD-induced intestinal permeability

The endocannabinoid system acts as a regulator of many functions in the body, including intestinal permeability.[8] Endocannabinoids are rapidly synthesised on demand, like in disease conditions, to activate cascade signalling via cannabinoid receptors.[25] Alcohol and high-fat diet (HFD) have been related to increased intestinal permeability.[26] Interestingly, pharmacological inhibition of CB1R ameliorates leaky gut and translocation of LPS. We therefore aimed at evaluating the role of intestinal CB1R in alcohol-induced and HFD-induced gut permeability using our mouse model of alcohol binge.[27] We first tested whether intestinal CB1R is implicated in alcohol-induced intestinal permeability by measuring *in vivo* permeability with the FITC-dextran 4 kDa probe in mice treated with the ethanol binge dose of 5 g/kg (mice metabolise alcohol 5-fold to 5.5-fold faster than humans).[28] We selected the dose of alcohol being administered in our binge model at 5 g/kg as previously described and the control groups received isocaloric dose of maltose (9 g/kg) (figure 2A). Remarkably, we revealed a significant improvement in intestinal permeability in male and female alcohol-treated CB1$^{IEC-/-}$ mice as compared with littermate CB1$^{f/f}$ wild-type mice (figure 2B).

A recent study by Cuddihey *et al* suggests that intestinal CB1R can also regulate HFD-induced leaky gut.[14] We therefore tested this hypothesis by feeding CB1$^{IEC-/-}$ male mice and littermate CB1$^{f/f}$ with HFD for 2 weeks to study the direct acute effects of the diet on intestinal permeability while avoiding the metabolic consequences of long-term HFD feeding, as previously described.[14] Our results revealed a decrease in HFD-induced intestinal permeability in CB1$^{IEC-/-}$ mice as compared with CB1$^{f/f}$ mice (figure 2C).

Given the involvement of CB1R in alcohol-induced intestinal permeability, we next evaluated whether alcohol binge alters endocannabinoids levels (figure 2D). Remarkably, we found increased levels of AEA, but not 2-AG, in the proximal small intestine in the mice post-alcohol binge (figure 2E).

Together, these results indicate that intestinal CB1R is implicated in alcohol-induced and HFD-induced increased intestinal permeability.

Villus differentiation mechanistically links inhibition of CB1R-ERK1/2 pathway and alcohol-induced intestinal permeability

Changes in villus differentiation and/or intestinal damage can cause increased intestinal permeability.[29] We therefore tested whether reduction in intestinal permeability was linked to one of these processes. Remarkably, duodenal histology and morphometric analyses showed that alcohol binge induced a reduction in villous length in CB1$^{f/f}$ mice. Alcohol-treated CB1$^{IEC-/-}$ mice had significantly longer villi compared with alcohol-treated
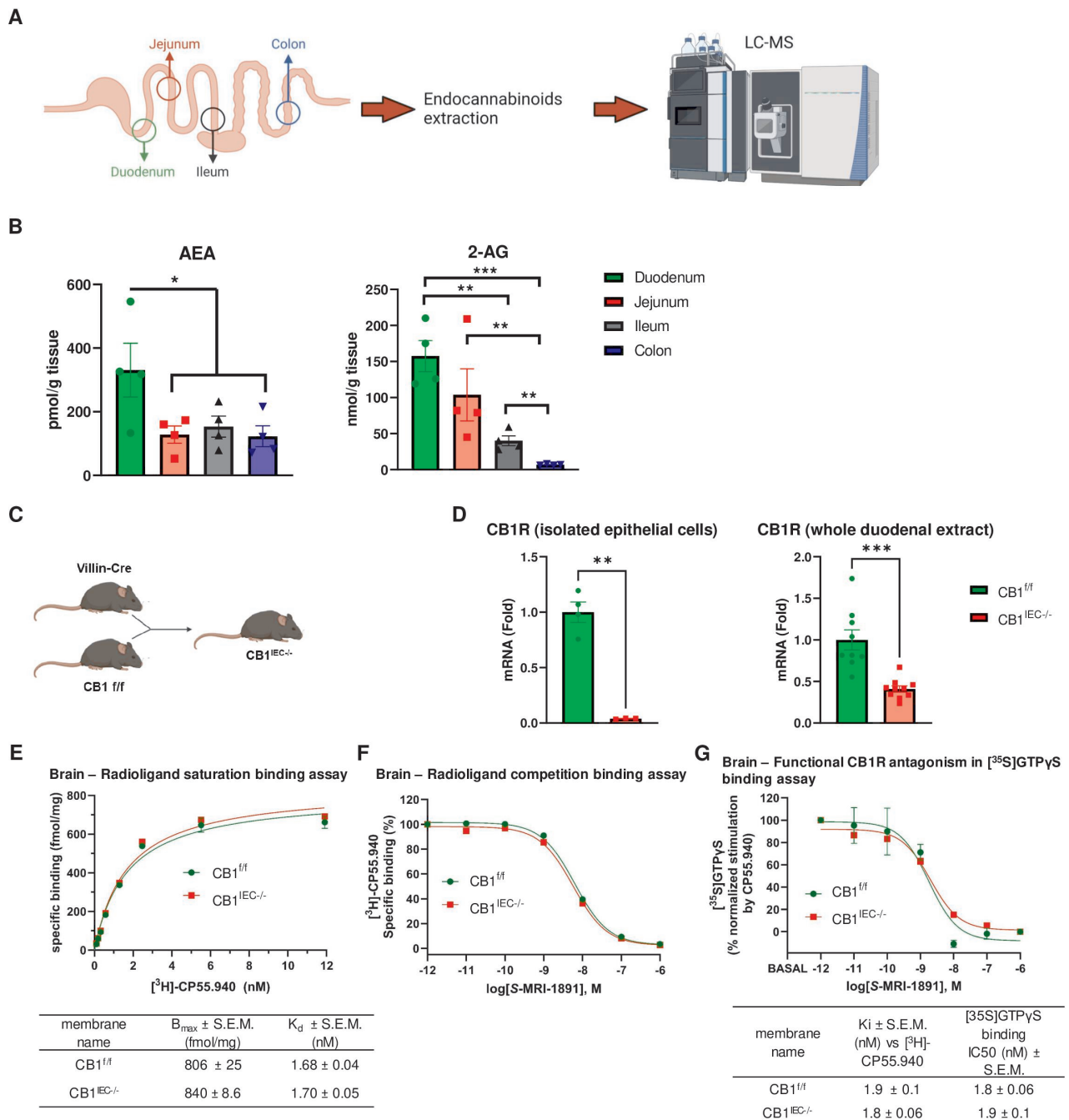
Figure 1 Measurement of gut endocannabinoids and generation of intestinal-specific CB1R KO mice. Different parts of the intestine were collected in C57BL/6J mice (n=4). Endocannabinoids were extracted and quantified by LC-MS/MS (created with Biorender.com) (A). Analysis of endocannabinoids in different segments of the intestine (B). Schematic of the crossing strategy between VillinCre and CB1[f/f] mice to obtain intestinal-specific CB1R KO mice (CB1[IEC−/−]) (C). Duodenal gene expression of CB1R in CB1[f/f] and CB1[IEC−/−] mice (D). Saturation binding of the tritiated antagonist [3H]-CP55,940 to wild-type CB1[f/f] and CB1[IEC−/−] mice brain membrane homogenate. Error bars represent SEM for three separate experiments, each performed in duplicate. The fitted K_d and B_{max} values are in the table below (E). CB1R binding affinity of the cannabinoid peripheral antagonist (S)-MRI-1891 in [3H]-CP55,940 competition binding assays to wild-type CB1[f/f] and CB1[IEC−/−] mice brain membrane homogenate. Figures represent the specific binding of the radioligand in percentage in the presence of increasing concentrations (10^{-12}–10^{-6} M) of the indicated ligand. Each experiment was performed in duplicate. Data are expressed as percentage of mean specific binding±SEM (n=3) (F). [35S]-GTPγS signal properties: inhibition of CB1R agonist (CP55,940)-induced [35S]-GTPγS binding by CB1R antagonist (S)-MRI-1891 using wild-type CB1[f/f] and CB1[IEC−/−] mice brain membrane homogenate. Values represent mean±SEM from three independent experiments. Below, binding affinity (K_i) and [35S]-GTPγS signal property IC_{50} of cannabinoid receptor antagonist (S)-MRI-1891 mice brain homogenate (G). Values represent mean±SEM; *p<0.05, **p<0.01, ***p<0.001. AEA, endocannabinoid anandamide; 2-AG, 2-arachidonoylglycerol; B_{max}, maximal number of binding sites; CB1[f/f], CB1 floxed/floxed; CB1[IEC−/−], intestinal epithelial-specific CB1R; CB1R, cannabinoid receptor 1; IC_{50}, inhibitory concentration; K_d, dissociation constant; KO, knockout; LC-MS/MS, liquid chromatography-tandem mass spectrometry; mRNA, messenger RNA.
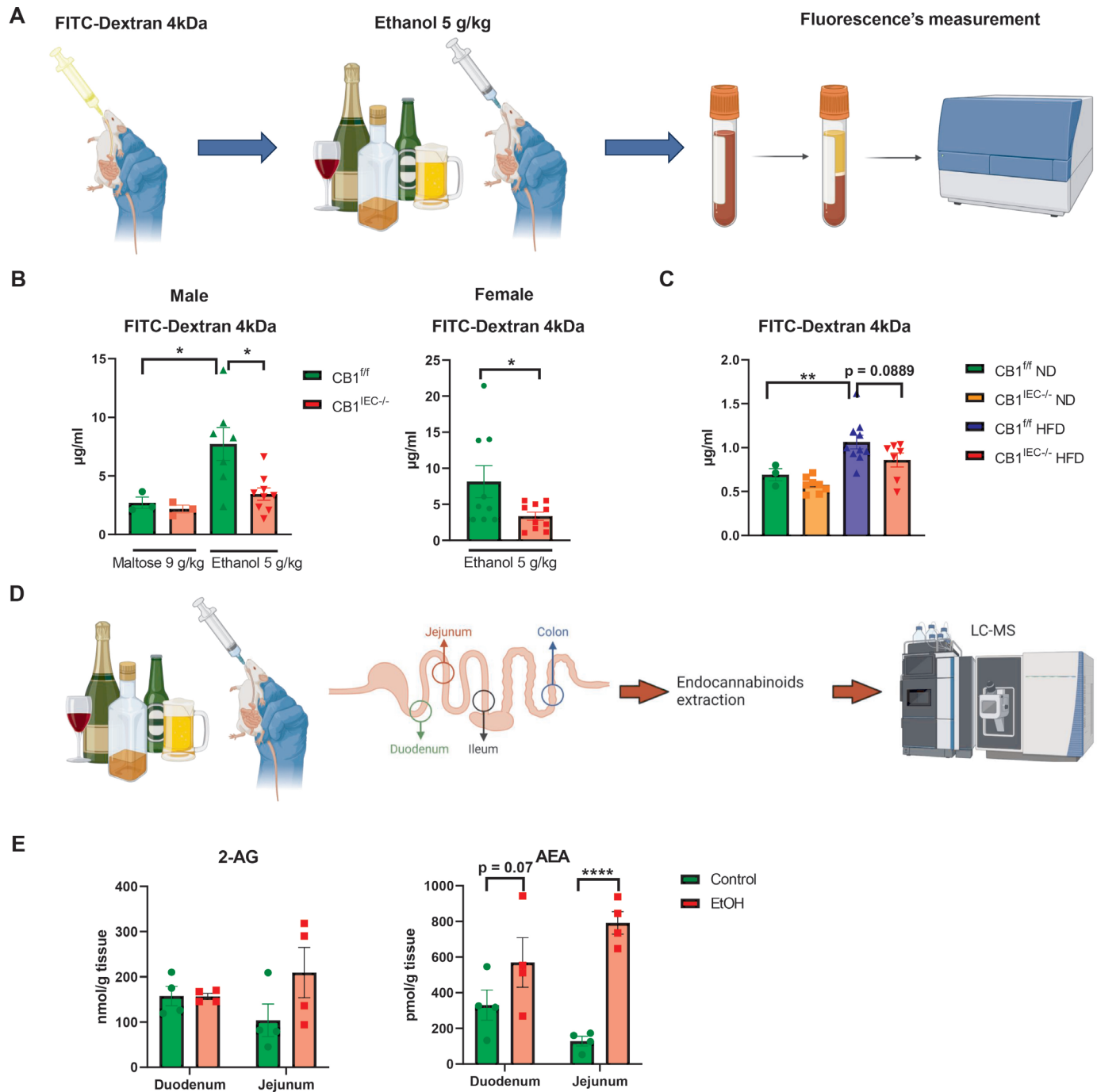
Figure 2 Intestinal CB1R and intestinal permeability. Schematic of the experimental protocol used to evaluate intestinal permeability *in vivo*. Mice were gavaged with the fluorescent probe FITC-dextran 4 kDa and binged with alcohol 5 g/kg 1 hour later. Control groups were treated with an isocaloric maltose solution of 9 g/kg (not shown in this representative schematic). Three hours later, blood was collected and centrifuged and fluorescence was measured in the plasma (created with Biorender. com) (A). Measurement of alcohol-induced intestinal permeability in male and female CB1$^{f/f}$ and CB1$^{IEC-/-}$ mice (n=3/group maltose, n=7–9/group ethanol in male, n=9–10/group female mice) (B). CB1$^{f/f}$ and CB1$^{IEC-/-}$ mice were randomly subjected to ND (n=4–8) and 60% HFD (n=7–10/group) for 2 weeks. After fasting overnight, mice were gavaged with FITC-dextran 4 kDa and intestinal permeability was measured (C). Different parts of the intestine were collected in C57BL/6 J mice (n=4/group) binged with alcohol versus control group. Endocannabinoids were extracted and quantified by LC-MS/MS (created with Biorender.com) (D). Analysis of endocannabinoids levels in alcohol-treated mice versus controls in the proximal small intestine (E). Values represent mean±SEM; *p<0.05, **p<0.01, ***p<0.001, ****p<0.0001. AEA, endocannabinoid anandamide; 2-AG, 2-arachidonoylglycerol; CB1$^{f/f}$, CB1 floxed/floxed; CB1$^{IEC-/-}$, intestinal epithelial-specific CB1R; CB1R, cannabinoid receptor 1; EtOH, ethanol; FITC, fluorescein isothicoyanate; HFD, high-fat diet; LC-MS/MS, liquid chromatography-tandem mass spectrometry; ND, normal chow diet.
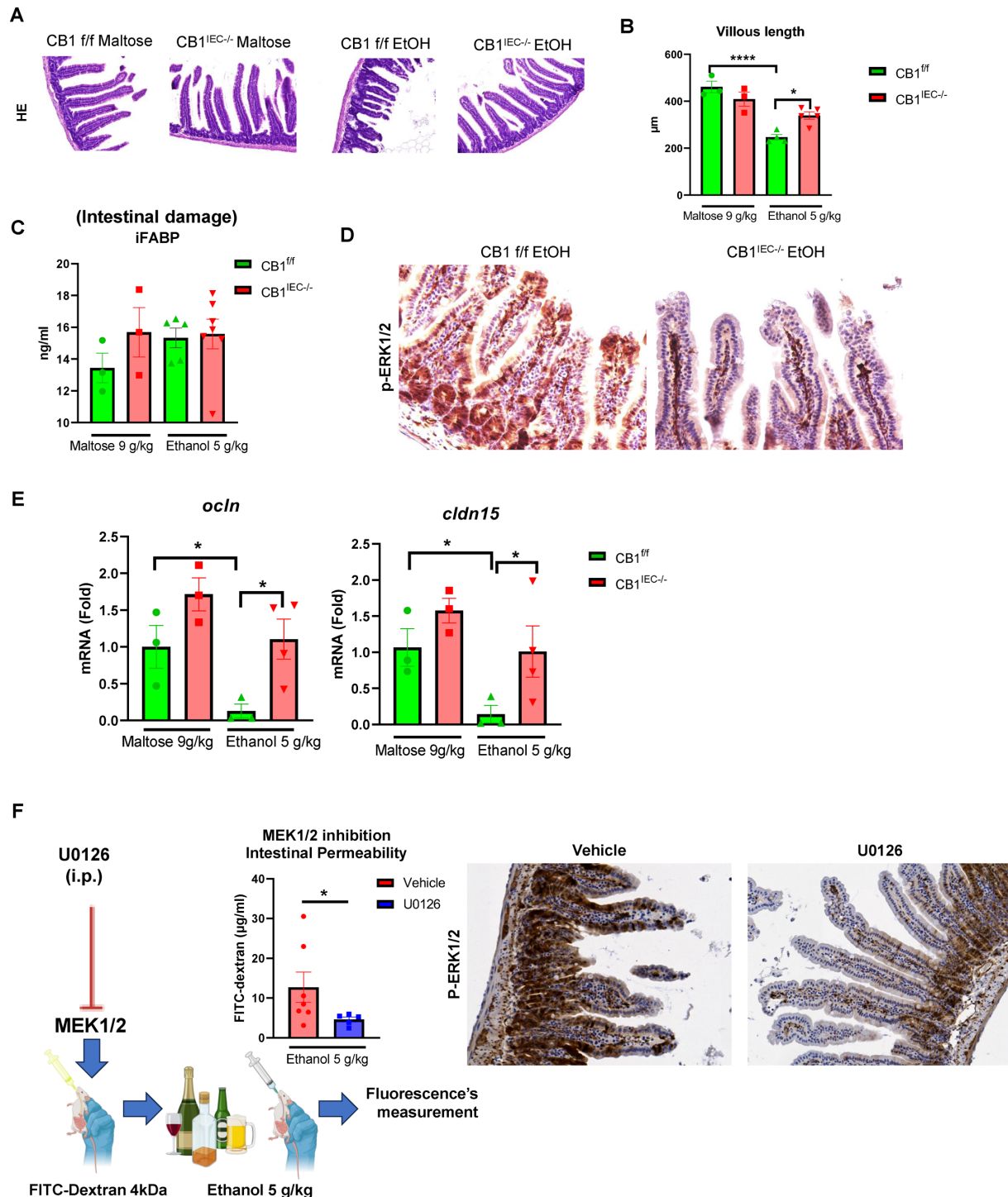
Figure 3 Differentiation, tight junctions and CB1R in alcohol-induced intestinal permeability. Hematoxylin & Eosin staining in CB1$^{f/f}$ and CB1$^{IEC-/-}$ mice treated with maltose or with ethanol (A). Morphometric analysis of villi length in the four groups of mice (n=3 to 5/group) (B). Serum iFABP, a marker of intestinal epithelial damage, in CB1$^{f/f}$ and CB1$^{IEC-/-}$ mice treated with maltose or with ethanol (n=3–7/group) (C). Immunohistochemistry staining of p-ERK1/2 in ethanol-treated CB1$^{f/f}$ and CB1$^{IEC-/-}$ mice (D). Duodenal gene expression of tight junctions ocln and cldn15 (n=3–4/group) (E). Mice were treated with vehicle or with the MEK1/2 inhibitor U0126 (n=5–7/group). Intestinal permeability was measured *in vivo* with the FITC-dextran 4 kDa method (figure created with Biorender.com). Duodenum was collected and stained with p-ERK1/2 antibody (F). Values represent mean±SEM; *p<0.05, **p<0.01, ***p<0.001, ****p<0.0001. CB1$^{f/f}$, CB1 floxed/floxed; CB1$^{IEC-/-}$, intestinal epithelial-specific CB1R; CB1R, cannabinoid receptor 1; cldn15, claudin 15; EtOH, ethanol; FITC, fluorescein isothicoyanate; iFABP, intestinal fatty acid binding protein; MEK, mitogen activated protein kinase kinase; mRNA, messenger RNA; ocln, occludin; pERK1/2, phosphorlated mitogen-activated protein kinase 1/2.

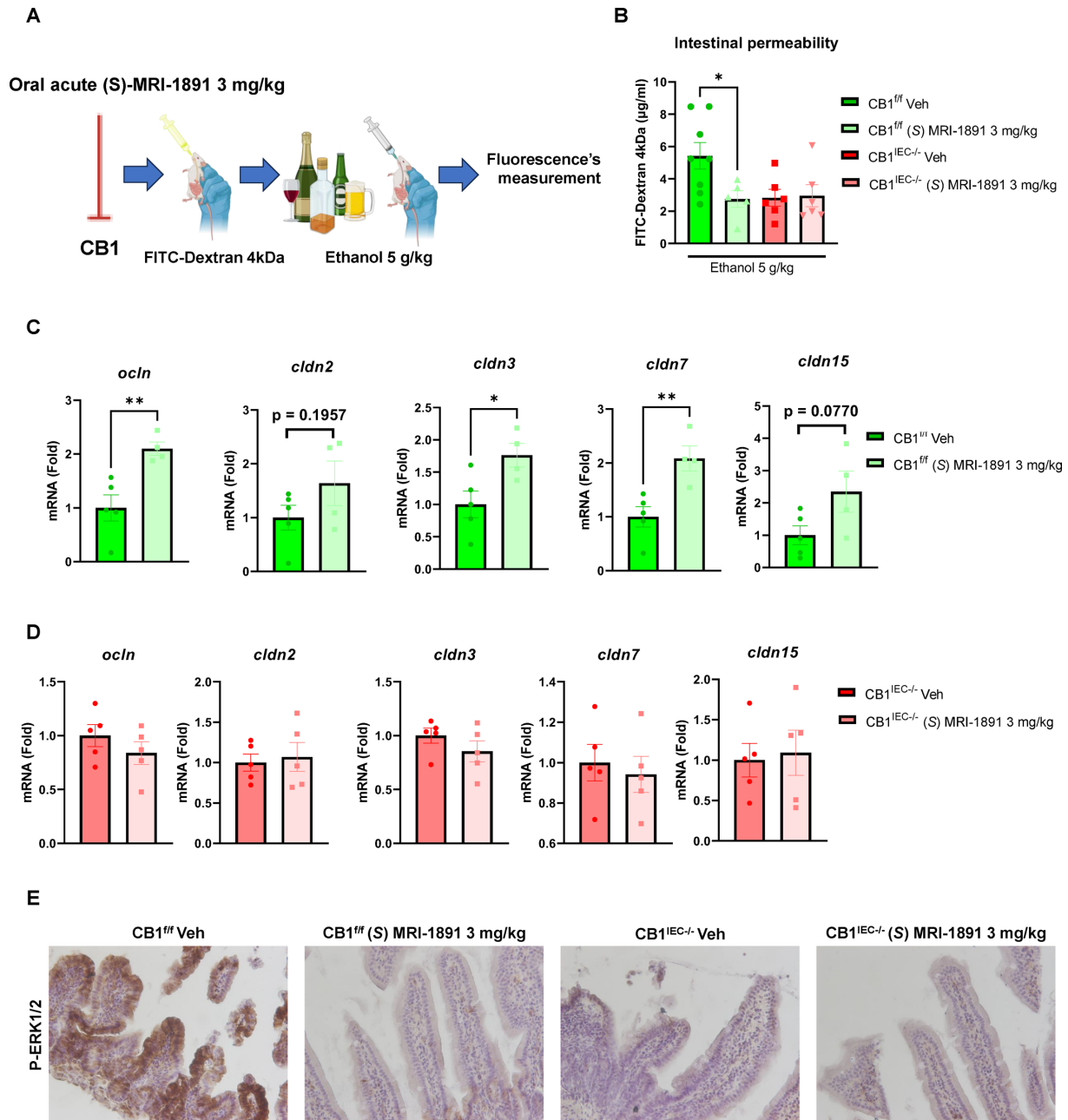**Figure 4** Pharmacological *in vivo* proof of the role of CB1R in alcohol-induced intestinal permeability. Mice (n=6–8/group) were treated orally by gavage with the peripheral-restricted CB1R selective antagonist (*S*)-MRI-1891 at the effective dose of 3 mg/kg. Intestinal permeability was assessed *in vivo* in ethanol-treated mice with the FITC-dextran 4 kDa method (figure created with Biorender.com) (A). Measurement of intestinal permeability in vehicle (Veh) and (*S*)-MRI-1891-treated CB1$^{f/f}$ and CB1$^{IEC-/-}$ mice (B). Duodenum tissues were collected, RNA extracted and gene expression of tight junctions-related genes ocln, cldn2, cldn3, cldn7 and cldn15 evaluated by RT-qPCR in CB1$^{f/f}$ (C) and CB1$^{IEC-/-}$ mice (D). Duodenal expression of p-ERK1/2 in vehicle and (*S*)-MRI-1891-treated CB1$^{f/f}$ and CB1$^{IEC-/-}$ mice (E). Values represent mean±SEM; *p<0.05, **p<0.01. CB1$^{f/f}$, CB1 floxed/floxed; CB1$^{IEC-/-}$, intestinal epithelial-specific CB1R; CB1R, cannabinoid receptor 1; cldn, claudin; FITC, fluorescein isothiocyanate; mRNA, messenger RNA; ocln, occludin; pERK1/2, phosphorlated mitogen-activated protein kinase 1/2; RT-qPCR, quantitative reverse transcription PCR.

littermate CB1$^{f/f}$ mice (figure 3A,B). By contrast, alcohol binge did not induce intestinal enterocyte damage (figure 3C), similar to what has been observed in human ABD.[4] CB1R signals to p-ERK1/2 activation, which has been implicated in the regulation of tight junction proteins and intestinal permeability.[30] Thus, we measured ERK1/2 activation and found that duodenal villi of

alcohol-treated CB1$^{IEC-/-}$ mice showed no expression of epithelial p-ERK1/2, in contrast to its high expression in CB1$^{f/f}$ mice (figure 3D). Moreover, gene expression of tight junction proteins occludin (ocln) and claudin 15 (cldn15) was markedly reduced in CB1$^{f/f}$ mice, while such reduction was restored to control levels in alcohol-treated CB1$^{IEC-/-}$ mice (figure 3E) in association with disrupted
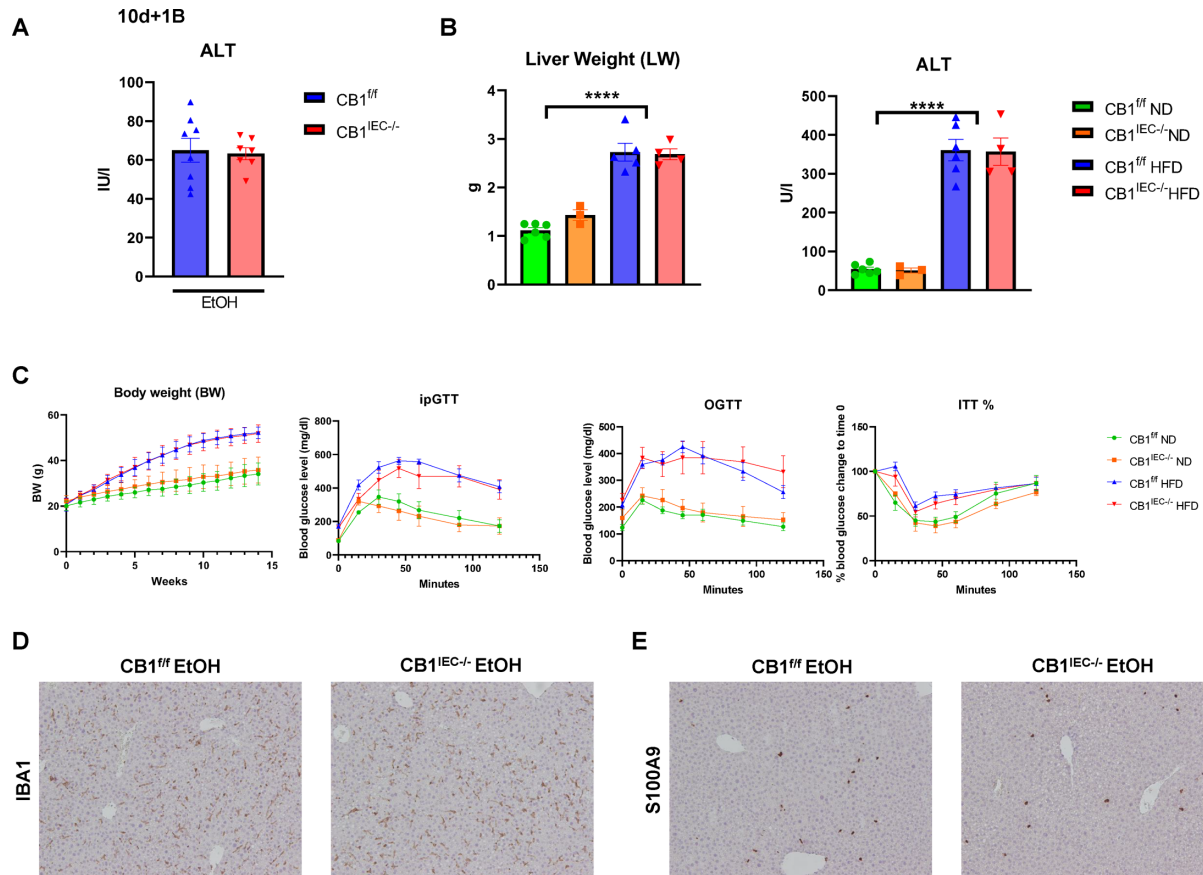
Figure 5 Intestinal CB1R in ALD and MASLD. CB1[f/f] and CB1[IEC−/−] mice (n=8/group) were subjected to the chronic-plus-binge (10d+1B) model. Serum ALT was measured as a marker of liver damage (A). CB1[f/f] and CB1[IEC−/−] mice (n=4–6/group) aged 6–8 weeks old were randomly fed with a ND or HFD for 14 weeks. Liver weight and ALT (B) as well as longitudinal body weight (BW) and ipGTT, OGTT and ITT (C) were measured. Representative staining of IBA1+ (macrophages) and S100A9+ (neutrophils) cells in livers from CB1[f/f] and CB1[IEC−/−] mice subjected to the 10d+1B model (D, E). Values represent mean±SEM; ****p<0.0001. ALD, alcohol-associated liver disease; ALT, alanine aminotransferase; CB1[f/f], CB1 floxed/floxed; CB1[IEC−/−], intestinal epithelial-specific CB1R; CB1R, cannabinoid receptor 1; EtOH, ethanol; HFD, high-fat diet; ipGTT, intraperitoneal glucose tolerance test; ITT, insulin tolerance test; MASLD, metabolic dysfunction-associated steatotic liver disease; ND, normal chow diet; OGTT, oral glucose tolerance test.

tight junction protein ZO-1 in alcohol-treated CB1[f/f] but not in CB1[IEC−/−] mice (online supplemental figure 1). These data suggest a link between CB1 signalling, p-ERK1/2 activation and regulation of tight junctions/intestinal permeability after alcohol binge. To mechanistically prove the role of p-ERK1/2 in alcohol-induced intestinal permeability *in vivo*, we treated wild-type mice with an MEK1/2 (upstream of p-ERK1/2) inhibitor, U0126, and measured intestinal permeability *in vivo*. Our results showed a significant reduction in intestinal permeability in mice treated with U0126 as compared with the vehicle (figure 3F), further supporting the implication of p-ERK1/2 in alcohol-induced leaky gut.

Pharmacological inhibition of intestinal CB1R restores intestinal barrier function

Our genetic approach supports the role of intestinal CB1R in the regulation of alcohol binge-induced intestinal permeability. To strengthen this hypothesis, we used peripheral-restricted selective CB1R antagonist

(*S*)-MRI-1891 (figure 4A). We selected the effective dose of 3 mg/kg, which fully antagonises CB1R *in vivo*.[21] Oral administration of (*S*)-MRI-1891 restored gut barrier function in CB1[f/f] control mice, in which intestinal CB1R is present, but did not change intestinal permeability *in vivo* in CB1[IEC−/−] mice, in which intestinal CB1R is absent (figure 4B). In accordance with the results of intestinal permeability, the treatment with (*S*)-MRI-1891 increased duodenal gene expression of tight junctions ocln, cldn3, cldn7 and cldn15 in CB1[f/f] mice (figure 4C) and did not change the expression of these genes in CB1[IEC−/−] (figure 4D), concomitantly with reduced p-ERK1/2 expression in CB1[f/f] mice treated with (*S*)-MRI-1891 (figure 4E), confirming the role of intestinal CB1R-ERK1/2 pathway in alcohol-induced intestinal permeability. One should note that, unlike intestinal epithelial-specific deletion of CB1R, (*S*)-MRI-1891 would also target other peripheral CB1R, including those in hepatocytes[31] and Kupffer cells,[32] chronic blockade of which may improve metabolic dysfunction-associated steatotic liver disease (MASLD)
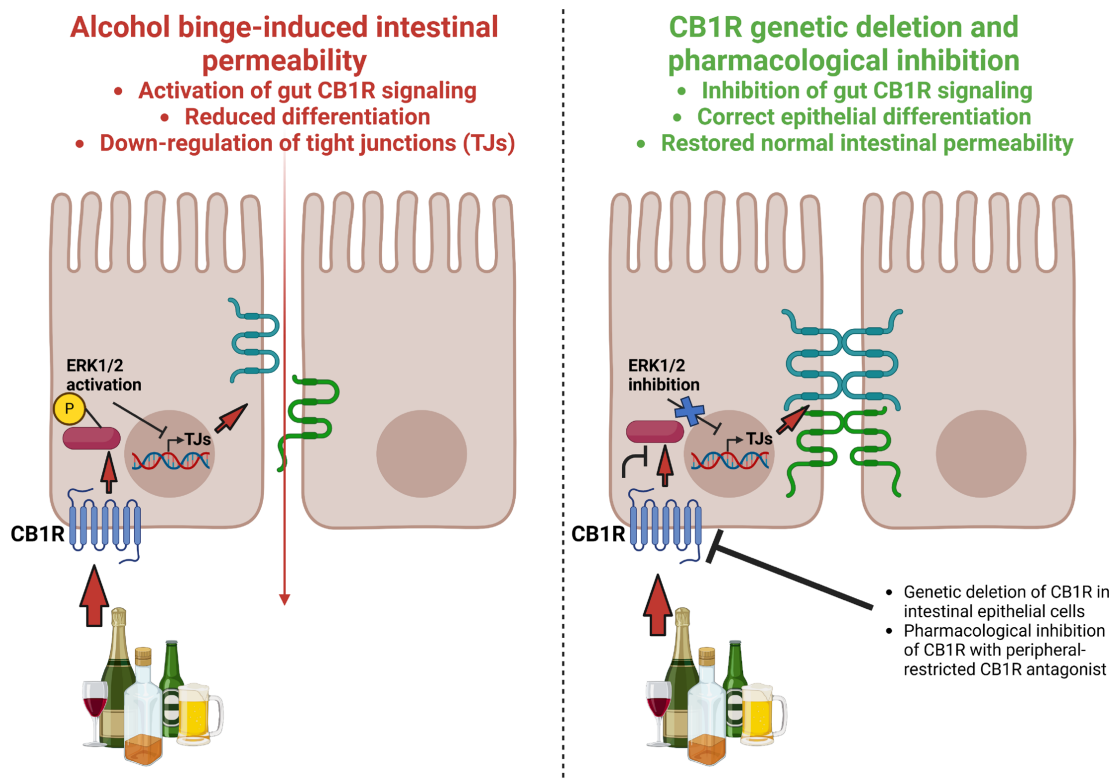
Figure 6 A schematic of the role of intestinal CB1R in alcohol-induced leaky gut. Alcohol binge increases intestinal permeability by activating intestinal epithelial CB1R-ERK1/2 signalling with subsequently reduced differentiation and downregulation of tight junctions (left). Genetic or pharmacological inhibition of intestinal CB1R-ERK1/2 signalling restored normal intestinal permeability and epithelial differentiation (right). Figure created with Biorender.com. CB1R, cannabinoid receptor 1; ERK1, mitogen-activated protein kinase 1/2.

by reducing hepatic triglyceride levels and improving hepatic insulin resistance, respectively.

Intestinal CB1R does not affect metabolic parameters nor improve ALD and MASLD

Many intestinal G protein-coupled receptors have been linked to body metabolism and utilisation of energy from carbohydrates and lipids.[33] Intestinal endocannabinoids and the CB1R are involved in the modulation of feeding behaviours.[34] However, it is not known whether intestinal CB1R plays a role in body metabolism. To test this, mice were placed in metabolic cages and metabolic parameters (eg, RQ, TEE, fat and carbohydrate oxidation) were measured by indirect calorimetry. Our results revealed similar metabolic profiles in CB1$^{IEC-/-}$ mice and wild-type littermate CB1$^{f/f}$ control mice (online supplemental figure 2), ruling out the role of gut CB1R in whole body metabolism.

The gut–liver axis has been linked to the development of both alcohol-associated liver disease (ALD) and MASLD.[35 36] As shown above, CB1$^{IEC-/-}$ mice had reduced alcohol-related and HFD-related leaky gut. We therefore tested whether reduction in intestinal permeability via genetic deletion of intestinal CB1R translated into less severe ALD and MASLD. The role of intestinal CB1R on ALD development was examined in the chronic-plus-binge model. Littermate CB1$^{f/f}$ and CB1$^{IEC-/-}$ mice were

acclimatised with a control liquid diet for 5 days and then fed with an ethanol diet for 10 days. On the 11th day, mice were treated by gavage with ethanol 5 g/kg and sacrificed 9 hours later.[37] Our results showed that alcohol-treated CB1$^{IEC-/-}$, despite reduced intestinal permeability, had similar liver damage as compared with CB1$^{f/f}$ mice (figure 5A).

We next tested whether intestinal CB1R regulates the development of MASLD. Littermate CB1$^{f/f}$ and CB1$^{IEC-/-}$ male mice 6–8 weeks old were randomly divided into normal diet (regular chow diet) and 60% HFD for 14 weeks and body weight was checked weekly. Our results showed similar liver weight in HFD-fed CB1$^{f/f}$ and CB1$^{IEC-/-}$ mice and in mice fed with normal diet (figure 5B), as well as similar body weight gain (figure 5C). We next measured intraperitoneal and oral glucose tolerance tests as well as insulin tolerance tests. We found no significant differences between CB1$^{f/f}$ and CB1$^{IEC-/-}$ mice fed with either HFD or normal diet, with clear differences between HFD and normal diet independent of the genotype (figure 5C). Similarly, there was no amelioration in liver damage in HFD-fed CB1$^{IEC-/-}$ mice as compared with CB1$^{f/f}$ mice (figure 5B). In addition, genetic deletion did not affect alcohol-induced liver inflammation (figure 5D).

Overall, our findings revealed that, although intestinal CB1 regulates alcohol-induced and HFD-induced

intestinal permeability, this effect has no significant influence on ALD and MASLD pathogenesis.

DISCUSSION

In this study, we have highlighted the role of gut CB1R in alcohol binge-induced intestinal permeability. Genetic deletion of intestinal epithelial CB1R and pharmacological inhibition of CB1R using the peripherally restricted CB1R antagonist (S)-MRI-1891 restored gut barrier function by inducing tight junction proteins and villus differentiation (figure 6). Our findings support the potential use of peripheral-restricted CB1R antagonists for the treatment of alcohol-induced leaky gut.

Our data revealed that alcohol binge activated CB1R signalling and led to reduced differentiation, downregulation of tight junctions and increased intestinal permeability. Deletion of intestinal CB1R completely prevented activation of ERK1/2 in the villi. Inhibiting ERK1/2 with the MEK1/2 inhibitor U0126 similarly improved gut barrier function. It is known that ERK1/2 is activated by a plethora of receptors. We were therefore surprised to see the complete abolishment of villus ERK1/2 activation in CB1$^{IEC-/-}$ mice. Despite low CB1R expression, we found that acute oral treatment with peripherally restricted CB1R antagonist (S)-MRI-1891 restored normal intestinal permeability in CB1$^{f/f}$ mice possibly by increasing gene expression of tight junction proteins. In addition, (S)-MRI-1891 did not have any effect on intestinal permeability in intestinal-specific CB1R knockout mice (CB1$^{IEC-/-}$), further proving that the effect seen for this antagonist was due to CB1R in the intestinal epithelium. The use of peripherally restricted CB1R antagonists was crucial to avoid central effects seen with antagonists that cross the blood–brain barrier, like rimonabant.[38]

The endocannabinoid system has been linked to different intestinal functions, such as gut motility, intestinal immunity, secretion of fluids and intestinal permeability.[8 9] CB2R receptors are only expressed in immune cells,[39] while CB1R is known to be highly expressed in the enteric nervous system.[40] Our data showed that deletion of intestinal epithelial CB1R accounts for around 50% of intestinal CB1R messenger RNA (mRNA), likely because the enteric nervous system accounts for the remaining half. Some reports suggest that epithelial CB1R expression is low, but is activated in several diseases, including inflammatory bowel disease and obesity.[14 41 42] In the current study, we confirmed that despite its low level of expression, intestinal epithelial CB1R signalling is clearly detectable. It is not entirely clear whether epithelial CB1R is expressed in the apical or basolateral membrane. A recent study showed that activation and inhibition of CB1R in vitro rely on the exposure of the compounds to the basolateral membrane.[43] The selectivity of the knockout was validated by the absence of change in CB1R expression or ligand binding in the brain. Moreover, our quantitative reverse transcription PCR (RT-qPCR) analysis

clearly demonstrated specific deletion of CB1R mRNA in intestinal epithelial cells from CB1$^{IEC-/-}$ mice.

Despite the positive effects on alcohol-induced and HFD-induced intestinal permeability, intestinal CB1R deficiency did not have significant effects on the development of both ALD and MASLD. Different pathways are implicated in the pathogenesis of steatotic liver diseases,[44–46] and leaky gut represents only one of these pathways. Moreover, we have recently demonstrated that paracellular intestinal permeability is not a prerequisite for microbial translocation to occur in patients with ALD.[47] Reduction of immune cells and defective gut immunosurveillance appear to be more critical processes in gut barrier dysfunction during ALD and MASLD than paracellular intestinal permeability alone.[4 45] In addition, changes in the microbiome and systemic inflammation also contribute to both ALD and MASLD.[35 36] It is therefore not surprising to us that selective targeting of CB1R in the intestine is not enough to improve liver function and metabolic parameters in ALD and MASLD, in which a multitarget approach is probably the best treatment option. Previous studies have shown that CB1R is expressed in cholecystokinin (CCK)-producing enteroendocrine cells as well as in K cells in the proximal small gut.[42] Our approach deletes CB1R in all intestinal epithelial cells, including K cells and CCK-producing cells. Despite the absence of epithelial CB1R in CB1$^{IEC-/-}$ mice, these animals gained similar body weight and had comparable glucose tolerance and insulin resistance with both chow diet and HFD compared with littermate control CB1$^{f/f}$. Many gut peptides as well as other organs contribute to the development of obesity and MASLD. It is therefore possible that deleting CB1R in some enteroendocrine cells is not enough to interfere with the complex MASLD pathogenesis.

In conclusion, our findings expand our understanding of the role of gut CB1R in the acute regulation of alcohol binge-induced intestinal permeability. We revealed that alcohol activates CB1R signalling with subsequent downregulation of tight junctions, thus leading to increased intestinal permeability. Genetic deletion of intestinal CB1R as well as pharmacological treatment with the peripherally restricted CB1R antagonist (S)-MRI-1891 were able to reverse this process, resulting in improved gut barrier function. Peripheral CB1R antagonism may be considered a novel therapeutic modality for treating leaky gut and its pathological consequences.

Author affiliations
[1]Laboratory of Liver Diseases, National Institute on Alcohol Abuse and Alcoholism, National Institutes of Health, Bethesda, Maryland, USA
[2]Laboratory of Physiologic Studies, National Institute on Alcohol Abuse and Alcoholism, National Institutes of Health, Bethesda, Maryland, USA
[3]Section on Fibrotic Disorders, National Institute on Alcohol Abuse and Alcoholism, National Institutes of Health, Bethesda, Maryland, USA
[4]Section on Medicinal Chemistry, National Institute on Alcohol Abuse and Alcoholism, National Institutes of Health, Bethesda, Maryland, USA
[5]Laboratory of Biomolecular Structure and Pharmacology, HUN-REN Biological Research Centre Szeged, Institute of Biochemistry, Szeged, Hungary

Patient and public involvement Patients and/or the public were not involved in the design, or conduct, or reporting, or dissemination plans of this research.

Patient consent for publication Not required.

Ethics approval All animals received humane care in accordance with the Guide for the Care and Use of Laboratory Animals published by the National Institutes of Health. Animal experiments were approved by the National Institute on Alcohol Abuse and Alcoholism (NIAAA) Animal Care and Use Committee (Animal Protocol LPS-GK-01 and LLD-BG-01).

Provenance and peer review Not commissioned; externally peer reviewed.

Data availability statement All data relevant to the study are included in the article or uploaded as supplementary information.

ORCID iDs
Luca Maccioni http://orcid.org/0009-0000-7580-3340
Szabolcs Dvorácskó http://orcid.org/0009-0000-7945-4061
Grzegorz Godlewski http://orcid.org/0009-0001-5489-0219
Resat Cinar http://orcid.org/0000-0002-8597-7253
Malliga R Iyer http://orcid.org/0000-0002-0116-4619
Bin Gao http://orcid.org/0000-0002-2505-2972
George Kunos http://orcid.org/0000-0003-1788-4976

REFERENCES

1 World Health Organization. Global Status Report on Alcohol and Health 2018. Vol 65. 2018.
2 Ding C, Ng Fat L, Britton A, *et al*. Binge-pattern alcohol consumption and genetic risk as determinants of alcohol-related liver disease. *Nat Commun* 2023;14:8041.
3 Fillmore MT, Jude R. Defining "binge" drinking as five drinks per occasion or drinking to a .08% BAC: which is more sensitive to risk? *Am J Addict* 2011;20:468–75.
4 Maccioni L, Fu Y, Horsmans Y, *et al*. Alcohol-associated bowel disease: new insights into pathogenesis. *eGastroenterology* 2023;1:e100013.
5 Khoshbin K, Camilleri M. Effects of dietary components on intestinal permeability in health and disease. *Am J Physiol Gastrointest Liver Physiol* 2020;319:G589–608.
6 Jew MH, Hsu CL. Alcohol, the gut microbiome, and liver disease. *J Gastroenterol Hepatol* 2023;38:1205–10.
7 Bruellman R, Llorente C. A Perspective Of Intestinal Immune-Microbiome Interactions In Alcohol-Associated Liver Disease. *Int J Biol Sci* 2021;17:307–27.
8 Cuddihey H, MacNaughton WK, Sharkey KA. Role of the Endocannabinoid System in the Regulation of Intestinal Homeostasis. *Cell Mol Gastroenterol Hepatol* 2022;14:947–63.
9 Lee Y, Jo J, Chung HY, *et al*. Endocannabinoids in the gastrointestinal tract. *Am J Physiol Gastrointest Liver Physiol* 2016;311:G655–66.
10 Izzo AA, Fezza F, Capasso R, *et al*. Cannabinoid CB1-receptor mediated regulation of gastrointestinal motility in mice in a model of intestinal inflammation. *Br J Pharmacol* 2001;134:563–70.
11 Fichna J, Bawa M, Thakur GA, *et al*. Cannabinoids alleviate experimentally induced intestinal inflammation by acting at central and peripheral receptors. *PLoS One* 2014;9:e109115.
12 DiPatrizio NV. Endocannabinoids and the Gut-Brain Control of Food Intake and Obesity. *Nutrients* 2021;13:1214.
13 Crowley K, Kiraga Ł, Miszczuk E, *et al*. Effects of Cannabinoids on Intestinal Motility, Barrier Permeability, and Therapeutic Potential in Gastrointestinal Diseases. *Int J Mol Sci* 2024;25:6682.
14 Cuddihey H, Cavin J-B, Keenan CM, *et al*. Role of CB$_1$ receptors in the acute regulation of small intestinal permeability: effects of high-fat diet. *Am J Physiol Gastrointest Liver Physiol* 2022;323:G219–38.
15 Santos-Molina L, Herrerias A, Zawatsky CN, *et al*. Effects of a Peripherally Restricted Hybrid Inhibitor of CB1 Receptors and iNOS on Alcohol Drinking Behavior and Alcohol-Induced Endotoxemia. *Molecules* 2021;26:5089.
16 González-Mariscal I, Montoro RA, Doyle ME, *et al*. Absence of cannabinoid 1 receptor in beta cells protects against high-fat/high-sugar diet-induced beta cell dysfunction and inflammation in murine islets. *Diabetologia* 2018;61:1470–83.
17 Godlewski G, Cinar R, Coffey NJ, *et al*. Targeting Peripheral CB$_1$ Receptors Reduces Ethanol Intake via a Gut-Brain Axis. *Cell Metab* 2019;29:1320–33.
18 Dvorácskó S, Keresztes A, Mollica A, *et al*. Preparation of bivalent agonists for targeting the mu opioid and cannabinoid receptors. *Eur J Med Chem* 2019;178:571–88.
19 Dvorácskó S, Herrerias A, Oliverio A, *et al*. Cannabinoformins: Designing Biguanide-Embedded, Orally Available, Peripherally Selective Cannabinoid-1 Receptor Antagonists for Metabolic Syndrome Disorders. *J Med Chem* 2023;66:11985–2004.
20 Wang L, Llorente C, Hartmann P, *et al*. Methods to determine intestinal permeability and bacterial translocation during liver disease. *J Immunol Methods* 2015;421:44–53.
21 Liu Z, Iyer MR, Godlewski G, *et al*. Functional Selectivity of a Biased Cannabinoid-1 Receptor (CB$_1$R) Antagonist. *ACS Pharmacol Transl Sci* 2021;4:1175–87.
22 Godlewski G, Jourdan T, Szanda G, *et al*. Mice lacking GPR3 receptors display late-onset obese phenotype due to impaired thermogenic function in brown adipose tissue. *Sci Rep* 2015;5:14953.
23 Simonson DC, DeFronzo RA. Indirect calorimetry: methodological and interpretative problems. *Am J Physiol* 1990;258:E399–412.
24 Shalon D, Culver RN, Grembi JA, *et al*. Profiling the human intestinal environment under physiological conditions. *Nature New Biol* 2023;617:581–91.
25 Kilaru A, Chapman KD. The endocannabinoid system. *Essays Biochem* 2020;64:485–99.
26 Tilg H, Adolph TE, Trauner M. Gut-liver axis: Pathophysiology concepts and clinical implications. *Cell Metab* 2022;34:1700–18.
27 Park SH, Seo W, Xu M-J, *et al*. Ethanol and its Nonoxidative Metabolites Promote Acute Liver Injury by Inducing ER Stress, Adipocyte Death, and Lipolysis. *Cell Mol Gastroenterol Hepatol* 2023;15:281–306.
28 Cederbaum AI. Alcohol metabolism. *Clin Liver Dis* 2012;16:667–85.
29 Bischoff SC, Barbara G, Buurman W, *et al*. Intestinal permeability--a new target for disease prevention and therapy. *BMC Gastroenterol* 2014;14:189.
30 Al-Sadi R, Guo S, Ye D, *et al*. TNF-α modulation of intestinal epithelial tight junction barrier is regulated by ERK1/2 activation of Elk-1. *Am J Pathol* 2013;183:1871–84.
31 Jeong W, Osei-Hyiaman D, Park O, *et al*. Paracrine activation of hepatic CB1 receptors by stellate cell-derived endocannabinoids mediates alcoholic fatty liver. *Cell Metab* 2008;7:227–35.
32 Jourdan T, Nicoloro SM, Zhou Z, *et al*. Decreasing CB$_1$ receptor signaling in Kupffer cells improves insulin sensitivity in obese mice. *Mol Metab* 2017;6:1517–28.
33 Cordomí A, Fourmy D, Tikhonova IG. Gut hormone GPCRs: structure, function, drug discovery. *Curr Opin Pharmacol* 2016;31:63–7.

34 DiPatrizio NV, Igarashi M, Narayanaswami V, *et al*. Fasting stimulates 2-AG biosynthesis in the small intestine: role of cholinergic pathways. *Am J Physiol Regul Integr Comp Physiol* 2015;309:R805–13.

35 Raya Tonetti F, Eguileor A, Mrdjen M, *et al*. Gut-liver axis: Recent concepts in pathophysiology in alcohol-associated liver disease. *Hepatology* 2024;80:1342–71.

36 Benedé-Ubieto R, Cubero FJ, Nevzorova YA. Breaking the barriers: the role of gut homeostasis in Metabolic-Associated Steatotic Liver Disease (MASLD). *Gut Microbes* 2024;16:2331460.

37 Bertola A, Mathews S, Ki SH, *et al*. Mouse model of chronic and binge ethanol feeding (the NIAAA model). *Nat Protoc* 2013;8:627–37.

38 Chorvat RJ. Peripherally restricted CB1 receptor blockers. *Bioorg Med Chem Lett* 2013;23:4751–60.

39 Acharya N, Penukonda S, Shcheglova T, *et al*. Endocannabinoid system acts as a regulator of immune homeostasis in the gut. *Proc Natl Acad Sci U S A* 2017;114:5005–10.

40 DiPatrizio NV. Endocannabinoids in the Gut. *Cannabis Cannabinoid Res* 2016;1:67–77.

41 Perisetti A, Rimu AH, Khan SA, *et al*. Role of cannabis in inflammatory bowel diseases. *Ann Gastroenterol* 2020;33:134–44.

42 Argueta DA, Perez PA, Makriyannis A, *et al*. Cannabinoid CB_1 Receptors Inhibit Gut-Brain Satiation Signaling in Diet-Induced Obesity. *Front Physiol* 2019;10:704.

43 Karwad MA, Couch DG, Theophilidou E, *et al*. The role of CB1 in intestinal permeability and inflammation. *FASEB J* 2017;31:3267–77.

44 Hutchison AL, Tavaglione F, Romeo S, *et al*. Endocrine aspects of metabolic dysfunction-associated steatotic liver disease (MASLD): Beyond insulin resistance. *J Hepatol* 2023;79:1524–41.

45 Sawada K, Chung H, Softic S, *et al*. The bidirectional immune crosstalk in metabolic dysfunction-associated steatotic liver disease. *Cell Metab* 2023;35:1852–71.

46 Mackowiak B, Fu Y, Maccioni L, *et al*. Alcohol-associated liver disease. *J Clin Invest* 2024;134:e176345.

47 Maccioni L, Gao B, Leclercq S, *et al*. Intestinal permeability, microbial translocation, changes in duodenal and fecal microbiota, and their associations with alcoholic liver disease progression in humans. *Gut Microbes* 2020;12:1782157.